ACS Macro Letters

Letter

Cite This: ACS Macro Lett. 2019, 8, 1068−1074

pubs.acs.org/macroletters

Palladium/Benzoic Acid-Catalyzed Regio- and Stereoselective Polymerization of Internal Diynes and Diols through C(sp^3)−H Activation

Jia Wang,[†] Tianwen Bai,[§] Yue Chen,[†] Canbin Ye,[†] Ting Han,[‡] Anjun Qin,*[,†] Jun Ling,*[,§] and Ben Zhong Tang*[,†,‡]

[†]State Key Laboratory of Luminescent Materials and Devices, Center for Aggregation-Induced Emission, South China University of Technology, Guangzhou 510640, China

[‡]Department of Chemistry, Hong Kong Branch of Chinese National Engineering Research Centre for Tissue Restoration and Reconstruction, Institute for Advanced Study, and Department of Chemical and Biological Engineering, The Hong Kong University of Science and Technology, Clear Water Bay, Kowloon, Hong Kong, China

[§]MOE Key Laboratory of Macromolecular Synthesis and Functionalization, Department of Polymer Science and Engineering, Zhejiang University, Hangzhou 310027, China

Supporting Information

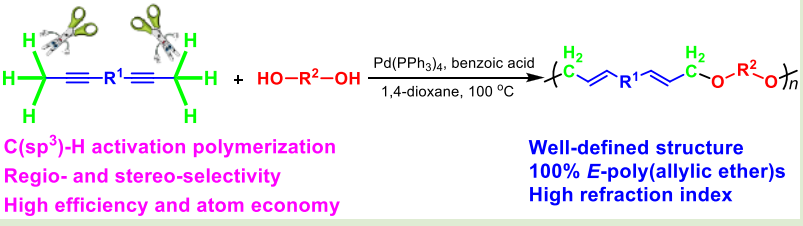

ABSTRACT: The C−H activation has been a hot research area in organic chemistry, and the most difficult one is the C(sp^3)−H activation. Although the C−H activation has been introduced to the research of synthetic polymer chemistry, the polymerization developed based on C(sp^3)−H activation is rarely reported, which will enrich the tools for the preparation of functional polymers. In this work, palladium/benzoic acid catalyzed polymerization of internal diynes and diols through C(sp^3)−H activation was successfully established. Regio- and stereoregular functional poly(allylic ether)s with 100% *E*-isomers and high weight average molecular weights (M_w up to 33200) were prepared in excellent yield (98%). The reaction mechanism was unveiled with the assistance of density functional theory calculations. Furthermore, the thin films of polymers display high refractive indices and low optical dispersions. The polymer containing tetraphenylethene moiety displays the aggregation-enhanced emission feature and could be used to generate 2D fluorescent photopattern. Thus, this work not only establishes a powerful polymerization based on C(sp^3)−H activation, but also furnishes functional polymers for diverse applications.

It is well-known that most nonrenewable fossil fuels are composed by the molecules containing C−C and C−H bonds. How to maximize the use efficiency and transfer them to advanced materials remains a great challenge.[1,2] One of the solutions is to actively cleave the C−H bond to generate functional C−X (X = C, N, O, S, ...) bond.[3,4] The C−H activation, created in the 1970s, holds the greatest merit that it could promote the reactivity of C−H bonds efficiently at a low temperature (<250 °C) comparing to traditional radical or carbocation reactions at elevated temperatures up to 800 °C.[5−7]

Theoretically, the C−H activation could be classified as C(sp)−H, C(sp^2)−H, and C(sp^3)−H ones according to the hybridized orbital of carbon atom.[8] Comparing to C(sp)−H and C(sp^2)−H bonds, the higher bond energies (90−100 kcal/mol) and lower acidity (pK_a: 45−60) of C(sp^3)−H bonds lead to their poorer reactivity.[9] Although C(sp^3)−H bonds are very inert, it does not mean they are impossible to be cleaved. Through unremitting efforts of organic chemists, elegant reaction systems capable of selectively activating C(sp^3)−H bonds have been developed.[10−13] In the reported methods, guiding groups are generally used to realize C(sp^3)−H activation. For example, Yamamoto and co-workers utilized carbon−carbon triple bonds to activate C(sp^3)−H bonds of methyl groups to enable them to react with alcohols, and regio- and stereoregular allylic ethers were furnished in excellent yields in the presence of a palladium/benzoic acid catalytic system.[14]

Notably, lots of C−H activation reactions are highly efficient and atom-economic and possess excellent regio- and stereoselectivity, thus, they could be regarded as a kind of "click"-like reaction. With the efforts paid by the polymer scientists, the

Received: June 12, 2019
Accepted: August 2, 2019
Published: August 13, 2019

DOI: 10.1021/acsmacrolett.9b00448
ACS Macro Lett. 2019, 8, 1068−1074

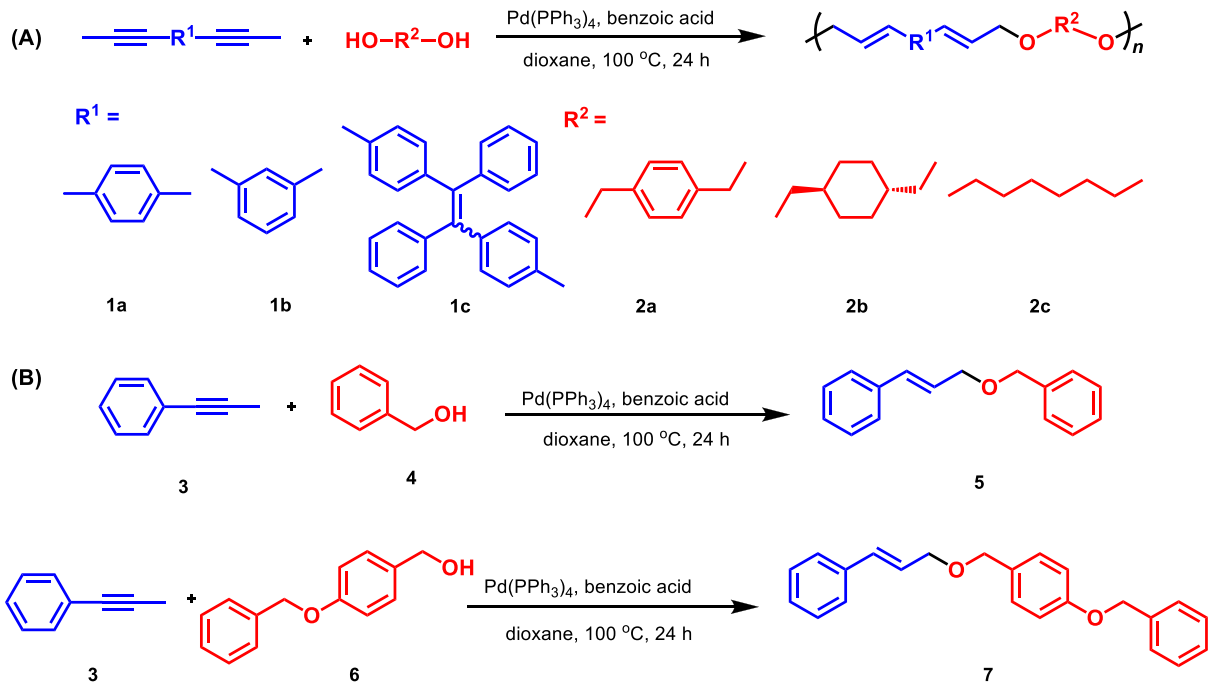

(C)

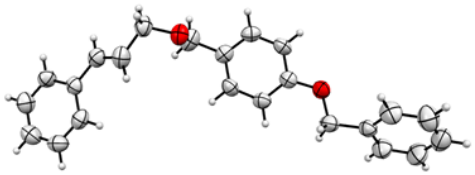

(D)

entry	monomer	polymer	yield (%)	M_w	PDI
1	**1a** + **2a**	P**1a2a**	98	21 200	2.40
2	**1a** + **2b**	P**1a2b**	95	17 200	2.41
3	**1a** + **2c**	P**1a2c**	77	9200	1.60
4	**1b** + **2a**	P**1b2a**	97	13 600	2.12
5	**1b** + **2b**	P**1b2b**	89	33 200	4.46
6	**1b** + **2c**	P**1b2c**	88	7300	1.65
7	**1c** + **2a**	P**1c2a**	83	11 300	2.61

Figure 1. (A) Palladium/benzoic acid-catalyzed polymerization of internal diynes **1** and diols **2**. (B) Synthetic routes to model compounds **5** and **7**. (C) ORTEP drawing of the crystal structure (CCDC 1521377) of model compound **7**. (D) Polymerization results of different monomers. The polymerization was carried out in 1,4-dioxane under nitrogen in the presence of $Pd(PPh_3)_4$ and benzoic acid at 100 °C for 24 h. [**1**] = [**2**] = 0.6 M, $[Pd(PPh_3)_4]/[\mathbf{1}]$ = 10%, [benzoic acid] = $2[Pd(PPh_3)_4]$.The molecular weights of polymers were estimated by advanced polymer chromatography (APC) using THF as an eluent on the basis of a polystyrene calibration; M_w = weight-average molecular weight; polydispersity index (PDI) = M_w/M_n; M_n = number-average molecular weight.

click reactions have been developed into click polymerizations.[15−18] Similarly, such C−H activation reactions well meet the requirements for developing into powerful and efficient polymerizations.[19−30] Indeed, the polymerization based on C−H activation have been reported in our groups. Three-component polymerizations of alkynes, aldehydes, and amines catalyzed by $InCl_3$ or CuCl via C(sp)−H activation were developed.[31,32] What's more, the C(sp^2)−H activation polymerization of alkyne and sulfonyldiphenol catalyzed by $Pd_2(dba)_3/AgAc_2/CuAc_2$ and bathophenanthroline was established by our group.[33] However, the polymerization based on C(sp^3)−H activation still faces great challenges.

In this work, we took this challenge and successfully established an efficient polymerization based on internal alkyne and alcohol monomers through the C(sp^3)−H activation (Figure 1A). A series of regio- and stereoregular poly(allylic ether)s with sole *E*-isomers and high weight-average molecule weights (M_w, up to 33200) were prepared in excellent yields (up to 98%). More importantly, our developed polymerization enjoys the advantage of atom economy over the Williamson ether synthesis or transetherification.[34] The resultant polymers possess good film-forming ability and show high refractive indices. Moreover, the polymerization is also tolerant to functional groups, and tetraphenylethene (TPE), a star molecule featured the aggregation-induced emission (AIE) characteristics,[35−38] could be facilely introduced into the polymer chains to endow the resultant polymers with aggregation-enhanced emission (AEE) features

In order to develop the C(sp^3)−H activation polymerization, the internal diynes **1** were readily synthesized by the methylation of terminal diynes with iodomethane (Schemes S1−S3), whereas, the diols **2** are commercially available. To establish a new polymerization, the optimization of reaction conditions is indispensable. Herein, we used diyne **1a** and diol **2a** as model monomers to perform the optimization (Figure 1A). The solvent, monomer concentration, catalyst loading ratio, reaction time, and temperature were carefully investigated (Tables S1−S5). All the factors exerted much effect on the polymerization. When the polymerization was carried out in 1,4-dioxane under nitrogen in the presence of Pd(0) and benzoic acid at 100 °C for 24 h ([**1a**] = [**2a**] = 0.6 M, [Pd(0)]/[**1a**] = 10%, [benzoic acid] = 2[Pd(0)]), the best results were obtained and the polymer with a M_w of 21200 was produced in 98% yield. By using the optimized conditions, we polymerize other internal diynes **1** and diols **2** to prove their universality (Figure 1A). The experimental results showed that all the polymerizations propagated smoothly and polymers with satisfactory M_w (7300−33200) could be obtained in good

DOI: 10.1021/acsmacrolett.9b00448
ACS Macro Lett. 2019, 8, 1068−1074

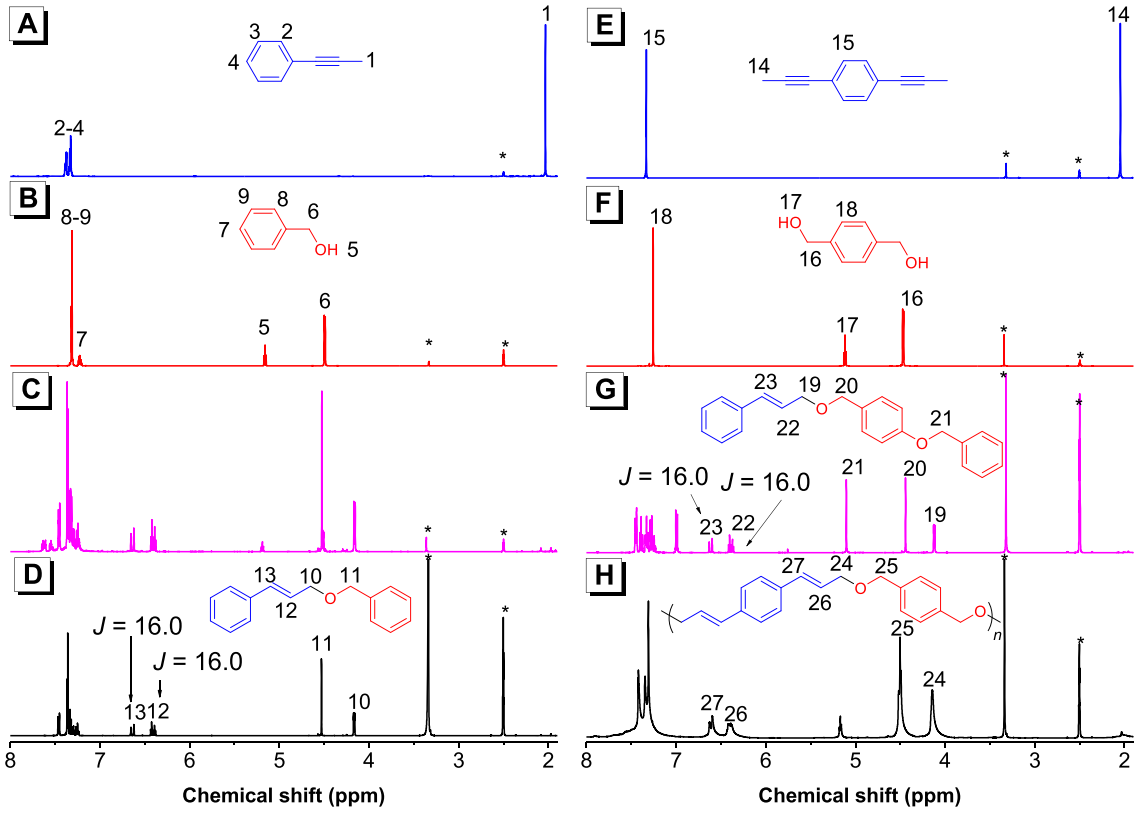

Figure 2. ^{1}H NMR spectra of alkyne **3** (A), alcohol **4** (B), crude model compound **5** (C), purified model compound **5** (D), **1a** (E), **2a** (F), model compound **7** (G), and P**1a2a** (H) in DMSO-d_6. The solvent peaks are marked with asterisks.

to excellent yields (77−98%; Figure 1D), further demonstrative of the robustness of our developed C(sp^3)−H activation polymerization. Moreover, the resultant polymers possess good thermal stability, and the temperatures (T_d) for 5% weight lost at a range from 248 to 326 °C under nitrogen, as evaluated by the thermogravimetric analysis (Figure S1).

To clearly characterize the structures of the resultant polymers, model compound **5** was designed and synthesized under the same conditions (Figure 1B). Its structure was also fully characterized. The ^{1}H NMR spectra of 1-phenyl-1-propyne **3** (Figure 2A), benzyl alcohol **4** (Figure 2B), and the crude model compound of **5** (Figure 2C) as well as the purified **5** (Figure 2D) are shown in Figure 2. The methyl protons adjacent to the ethynyl group of **3** and hydroxyl proton of **4** resonated at δ 2.04 and 5.12, respectively, and disappeared in the spectrum of **5**. Meanwhile, new peaks at δ 6.65, 6.42, 4.53, and 4.17, assignable to the proton resonances of the newly formed Ar−C***H***=CH, CH=C***H***−CH_2, O−C***H***$_2$−Ar, and CH=CH−C***H***$_2$, respectively, appeared in the spectrum of **5**. The coupling constants (J) of vinyl protons were deduced to be 16.0 Hz, suggesting that **5** adopts an *E*-configuration. It is worth noting that no resonance assignable to the *Z*-allylic ether was observed in the ^{1}H NMR spectrum of the crude product of **5**, indicating that this reaction is stereoselective. To collect a direct proof for the regularity of the product, another solid model compound of **7** with a larger molecular size was designed and synthesized (Figure 1B and Scheme S4), because **5** is oil, which is impossible to grow single crystals for structural analysis. Compound **7** was yielded as a solid, and its ^{1}H NMR spectrum showed the same results as **5** (Figure 2G). Delightfully, we successfully got its single crystals, and the analysis showed that the hydrogen atoms are arranged on the opposite side of the vinyl group (Figure 1C), further manifesting that the model compounds enjoy 100% *E*-stereoregularity.

Next, we characterized the structures of the resultant polymers and satisfactory analysis data were obtained. Herein, the FT-IR and NMR spectra of **1a**, **2a**, and P**1a2a** are shown as examples, while those of other compounds and polymers are given in Figures S2−S21. The FT-IR spectra of **1a**, **2a**, and P**1a2a** are provided in Figure 3. The absorption of **1a**

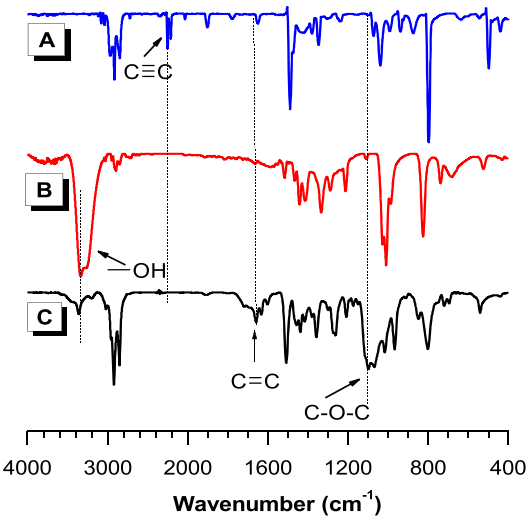

Figure 3. FT-IR spectra of **1a** (A), **2a** (B), and P**1a2a** (C).

DOI: 10.1021/acsmacrolett.9b00448
ACS Macro Lett. 2019, 8, 1068−1074

associating with C≡C stretching vibration was observed at 2245 cm^{-1}, and the −OH stretching vibration of **2a** emerged at 3400 cm^{-1}. In the spectrum of P**1a2a**, the former disappeared and the latter became very weak. Meanwhile, new peaks of the C−O and C═C stretching vibrations of allylic ether appeared at 1098 and 1659 cm^{-1}, respectively. These results indicated that almost all C≡C and −OH groups in **1a** and **2a** had been consumed by the polymerization.

The ^{1}H NMR spectra of **1a**, **2a**, **7**, and P**1a2a** could provide more detailed information (Figure 2E−H). The methyl protons adjacent to the ethynyl groups of **1a** resonated at δ 2.04 disappeared in the spectrum of P**1a2a**. Meanwhile, new peaks at δ 6.62, 6.41, 4.50, and 4.14, assignable to the proton resonances of the newly formed Ar−C***H***═CH, CH═C***H***−CH_2, O−C***H***$_2$−Ar, and CH═CH−C***H***$_2$, respectively, appeared in the spectrum of P**1a2a**. Moreover, the profile of the ^{1}H NMR spectrum of P**1a2a** is very similar to those of model compounds **5** and **7**, indicating that the polymerization via C(sp^3)−H activation could generate poly(allylic ether)s with 100% *E*-isomers. Notably, in the spectrum of P**1a2a**, the peak resonated at δ 5.12 was assignable to the hydroxyl proton for it could be vanished after adding a drop of D_2O in DMSO-d_6 solution, which verified that P**1a2a** is terminated by the −OH groups (Figure S14). The ^{13}C NMR analysis also provides persuasive information about the polymer structures (Figure S15). The characteristic carbon resonances of **C**≡**C**−**C**H_3 of **1a** were clearly observed at δ 88.36, 79.31, and 3.93, respectively, which disappeared in the spectra of **5** and P**1a2a**. Meanwhile, new peaks at δ 71.21 and 70.09 assignable to the resonances of the newly formed CH═CH−**C**H_2 and O−**C**H_2−Ar, respectively, appeared in the spectra of **5** and P**1a2a**, indicative of the complete consumption of ethynyl groups and the accomplishment of the polymerization.

To fully understand the regio- and stereoselectivity of this polymerization, the theoretical calculation using the density functional theory (DFT) method was performed. To simplify the calculation, 1-phenyl-1-propyne and benzyl alcohol as model reaction molecules were adopted. According to DFT calculations, the coupling process catalyzed with a Pd complex consists of three main steps, that is, electrophilic addition on an ethnynyl group, elimination, and electrophilic addition on the formed allene group, as shown in Figure 4A with selected 3D geometries (Figure S24) and coordinates in the Supporting Information. After coordinating with 1-phenyl-1-propyne, electrophilic addition on an ethynyl group is confirmed via a four-member ring transition state (**TS1**) with negligible ΔG = 1.36 kcal/mol. Since the Pd−H bond has broken up, the nucleophilic Pd−X center migrated to β-C and further induced elimination of the proton on γ-C (**TS2**) with ΔG = 10.81 kcal/mol, which released an allene compound **III** with a C═C bond length of 1.31 Å (α-C to β-C) and 1.36 Å (β-C to γ-C).

The regio- and *Z*/*E*-selective addition of benzyl alcohol is worthy of noticing in the electrophilic addition step on allene groups. Compared with ethynyl groups, electron density located on allene is lower, which leads to a higher addition ΔG barrier (>30 kcal/mol) as the rate-determining step in the whole process. According to DFT calculations, β-C is confirmed with lower nucleophilic properties (charge: −0.57, Mulliken) than α-C (−0.27) and γ-C (−0.07), causing a higher addition energy barrier when oxygen is added at the β-C position (**TS3_C2**), as shown in Figure 4B. When oxygen is added at the γ-C position, the *Z*/*E* configuration is also examined (**TS3_C3** and **TS3_C3Z**). According to calculation

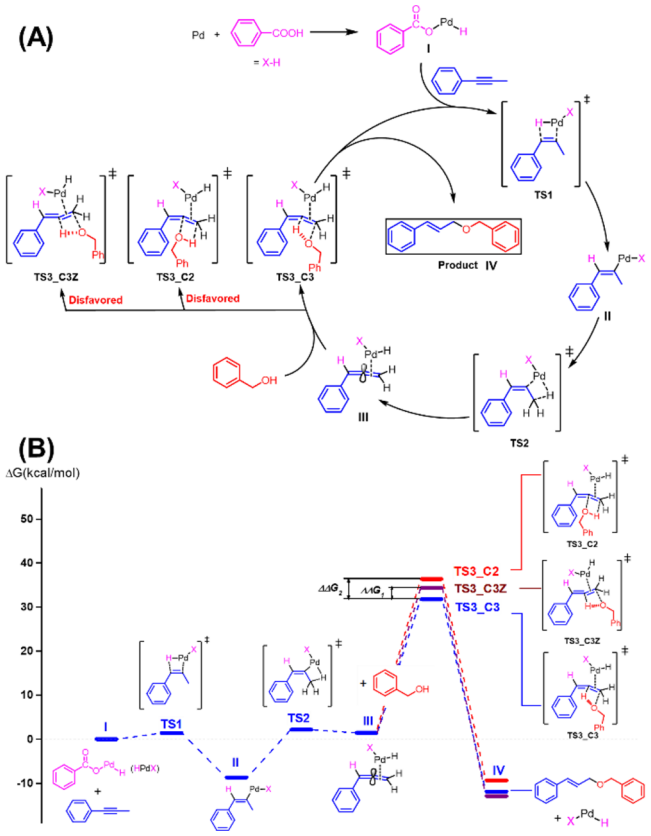

Figure 4. (A) Proposed reaction mechanism according to DFT calculations. (B) DFT calculated profiles of the whole process of all intermediates and TSs. The difference of Gibbs free energy barriers of **TS3_C3Z** ($\Delta\Delta G_1$ = 2.56 kcal/mol) and **TS3_C2** ($\Delta\Delta G_2$ = 4.31 kcal/mol) compared with **TS3_C3** is estimated under tight criteria of M06-2X/6-311++G(d,p) for light atom and SDD for Pd.

results, γ-C addition with the *E*-configuration is preferred with the lowest energy barrier (ΔG = 30.37 kcal/mol, **III** to **TS3_C3**) compared with **TS3_C3Z** ($\Delta\Delta G_1$ = 2.56 kcal/mol) and **TS3_C2** ($\Delta\Delta G_2$ = 4.31 kcal/mol), producing the *E*-configuration product **IV** and isolated Pd complex for the next cycle.

Afterward, we investigated the properties of the resultant polymers. All the polymers are emissive, and the absolute fluorescence quantum yields range from 0.3 to 3.2% (Table S7). P**1c2a**, containing the moiety of TPE, is expected to possess the AIE feature.[39−41] As shown in Figure 5A, upon excitation with the maximum absorption wavelength of 337 nm (Figure S23), the THF solution of P**1c2a** emits gently with a peak at 499 nm. However, addition of a poor solvent of water into its THF solution gradually enhanced its emission without a noticeable change on the emission profiles, and emission intensity in the THF/water mixture with f_w of 90% is about 4.4× higher than that of THF solution (Figure 5B), demonstrating the unique aggregation-enhanced emission (AEE) characteristics.[42]

Our resultant polymers contain many highly polarized aromatic rings and oxygen atoms, which might be beneficial to achieve a high refractive index (RI).[43,44] As shown in Figure 6A, the polymer films possess high RI values in the range of 1.6111−1.6840 at the wavelength of 632.8 nm (Table S7). It is worth noting that these values are much higher than those of the commercial optical plastics such as polyacrylate (1.492),

DOI: 10.1021/acsmacrolett.9b00448
ACS Macro Lett. 2019, 8, 1068−1074

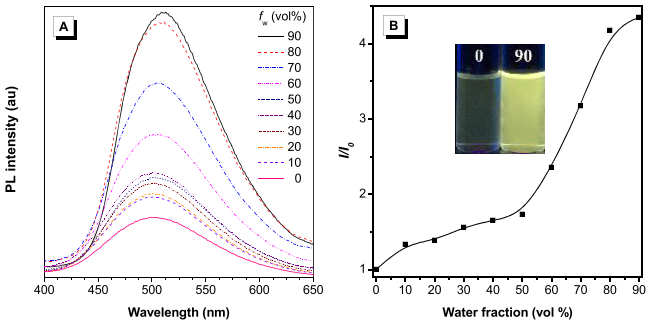

Figure 5. (A) Photoluminescent spectra of P**1c2a** in THF/water mixture with different water fractions (f_w, vol %). (B) Plot of relative intensity of P**1c2a** vs f_w. I_0 and I are the maximal emission intensity recorded before and after addition of water into the THF solution of P**1c2a**. Concentration of polymers = 10 μM, λ_{ex} = 337 nm. Inset: photograph of P**1c2a** in THF/water mixture with f_w of 0 and 90% taken under a UV lamp peaked at 365 nm.

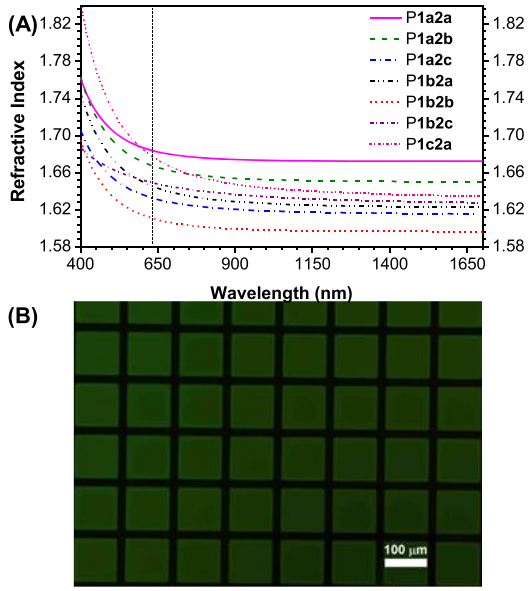

Figure 6. (A) Light refraction spectra of thin solid films of resultant polymers. (B) Two-dimensional fluorescent photopattern generated by UV irradiation of a thin film of P**1c2a** in air. The photograph was taken under a UV lamp peaked at 365 nm.

polystyrene (1.587), polycarbonate (1.580), and poly(methyl methacrylate) (1.489) at the same wavelength.[45] What's more, all the polymers had small chromatic dispersion values (0.0287−0.0941) and modified chromatic dispersion values (0.0009−0.0256). Owning to its good film-forming ability, unique AEE features, and the vinyl groups, P**1c2a** could be used to fabricate fluorescent 2D patterns (Figure 6B). After irradiation under a UV lamp at 365 nm in air for 10 min through a copper photomask, the exposed region (dark line) of thin film of P**1c2a** on silicon wafer shows no emission probably due to UV-induced oxidation in air. While, the left parts (yellow green squares) retain the intense emission. Thus, a 2D fluorescent pattern with sharp edges was facilely generated. These merits of poly(allylic ether)s imply their potential applications as optical materials.

In summary, we successfully developed a new palladium/benzoic acid-catalyzed polymerization via C(sp^3)−H activation of internal diynes and diols. Regio- and stereoregular functional poly(allylic ether)s with high M_w (up to 33200) were generated in excellent yields (up to 98%). And DFT calculations have unveiled the underlying reaction mechanism of this C(sp^3)−H activation polymerization. The resultant polymers possess excellent film-forming ability and show high refractive indices in the range of 1.6111−1.6840 at 632.8 nm and low optical dispersions. Furthermore, the poly(allylic ether) bearing TPE group showed unique AEE characteristics and could be used to fabricate a 2D photopattern. Thus, this work not only provides the first example of using C(sp^3)−H activation to establish a new powerful polymerization of diynes and diols, but also generates a series of regio- and stereoregular poly(allylic ether)s with versatile properties for diverse applications.

■ ASSOCIATED CONTENT

Supporting Information

The Supporting Information is available free of charge on the ACS Publications website at DOI: 10.1021/acsmacrolett.9b00448.

Materials, instrumentation, experimental procedures, characterization data and calculation details; polymerization condition optimization on solvent, monomer concentration, catalyst loading, reaction time, and temperature; ^{1}H and ^{13}C NMR and FT-IR spectra of monomers and polymers; and UV−vis absorption spectra of polymers in THF (PDF)

■ AUTHOR INFORMATION

Corresponding Authors

*E-mail: msqinaj@scut.edu.cn.
*E-mail: lingjun@zju.edu.cn.
*E-mail: tangbenz@ust.hk.

ORCID

Ting Han: 0000-0003-1521-6333
Anjun Qin: 0000-0001-7158-1808
Jun Ling: 0000-0002-0365-1381
Ben Zhong Tang: 0000-0002-0293-964X

Notes

The authors declare no competing financial interest.

■ ACKNOWLEDGMENTS

This work was financially supported by the National Natural Science Foundation of China (21788102, 21525417, and 21490571); the Natural Science Foundation of Guangdong Province (2019B030301003 and 2016A030312002); the Fundamental Research Funds for the Central Universities (2015ZY013); and the Innovation and Technology Commission of Hong Kong (ITC-CNERC14S01).

■ REFERENCES

(1) Bergman, R. G. Organometallic Chemistry: C−H Activation. *Nature* **2007**, *446*, 391−393.
(2) Yang, Y.; Wang, C. Direct Silylation Reactions of Inert C-H Bonds via Transition Metal Catalysis. *Sci. China: Chem.* **2015**, *58*, 1266−1279.
(3) Chen, X.; Engle, K. M.; Wang, D. H.; Yu, J. Q. Palladium(II)-Catalyzed C−H Activation/C−C Cross-Coupling Reactions: Versatility and Practicality. *Angew. Chem., Int. Ed.* **2009**, *48*, 5094−5115.
(4) Davies, H. M. L.; Du Bois, J.; Yu, J. Q. C−H Functionalization in Organic Synthesis. *Chem. Soc. Rev.* **2011**, *40*, 1855−1856.

DOI: 10.1021/acsmacrolett.9b00448
ACS Macro Lett. 2019, 8, 1068−1074

(5) Labinger, J. A.; Bercaw, J. E. Understanding and Exploiting C−H Bond Activation. *Nature* **2002**, *417*, 507−514.
(6) Wang, X.; Truesdale, L.; Yu, J. Q. Pd(II)-Catalyzed ortho-Trifluoromethylation of Arenes Using TFA as a Promoter. *J. Am. Chem. Soc.* **2010**, *132*, 3648−3649.
(7) Zhang, Z.; Tanaka, K.; Yu, J. Q. Remote Site-Selective C−H Activation Directed by a Catalytic Bifunctional Template. *Nature* **2017**, *543*, 538−542.
(8) Wencel-Delord, J.; Droge, T.; Liu, F.; Glorius, F. Towards Mild Metal-Catalyzed C−H Bond Activation. *Chem. Soc. Rev.* **2011**, *40*, 4740−4761.
(9) He, J.; Wasa, M.; Chan, K. S. L.; Shao, Q.; Yu, J. Q. Palladium-Catalyzed Transformations of Alkyl C−H Bonds. *Chem. Rev.* **2017**, *117*, 8754−8786.
(10) Shang, R.; Ilies, L.; Matsumoto, A.; Nakamura, E. β-Arylation of Carboxamides via Iron-Catalyzed C(sp^3)−H Bond Activation. *J. Am. Chem. Soc.* **2013**, *135*, 6030−6032.
(11) Wu, Q. F.; Shen, P. X.; He, J.; Wang, X. B.; Zhang, F.; Shao, Q.; Zhu, R.-Y.; Mapelli, C.; Qiao, J. X.; Poss, M. A.; Yu, J.-Q. Formation of α-Chiral Centers by Asymmetric β-C(sp^3)−H Arylation, Alkenylation, and Alkynylation. *Science* **2017**, *355*, 499−503.
(12) Li, H.; Gontla, R.; Flegel, J.; Merten, C.; Ziegler, S.; Antonchick, A. P.; Waldmann, H. Enantioselective Formal C(sp^3)−H Bond Activation in the Synthesis of Bioactive Spiropyrazolone Derivatives. *Angew. Chem., Int. Ed.* **2019**, *58*, 307−311.
(13) Zhu, Y.; Huang, K.; Pan, J.; Qiu, X.; Luo, X.; Qin, Q.; Wei, J.; Wen, X.; Zhang, L.; Jiao, N. Silver-Catalyzed Remote Csp^3−H Functionalization of Aliphatic Alcohols. *Nat. Commun.* **2018**, *9*, 2625.
(14) Kadota, I.; Lutete, L. M.; Shibuya, A.; Yamamoto, Y. Palladium/Benzoic Acid-Catalyzed Hydroalkoxylation of Alkynes. *Tetrahedron Lett.* **2001**, *42*, 6207−6210.
(15) Kolb, H. C.; Finn, M. G.; Sharpless, K. B. Click Chemistry: Diverse Chemical Function from a Few Good Reactions. *Angew. Chem., Int. Ed.* **2001**, *40*, 2004−2021.
(16) He, B.; Su, H.; Bai, T.; Wu, Y.; Li, S.; Gao, M.; Hu, R.; Zhao, Z.; Qin, A.; Ling, J.; Tang, B. Z. Spontaneous Amino-yne Click Polymerization: A Powerful Tool toward Regio- and Stereospecific Poly(β-aminoacrylate)s. *J. Am. Chem. Soc.* **2017**, *139*, 5437−5443.
(17) Huang, D.; Liu, Y.; Qin, A.; Tang, B. Z. Structure−Property Relationship of Regioregular Polytriazoles Produced by Ligand-Controlled Regiodivergent Ru(II)-Catalyzed Azide−Alkyne Click Polymerization. *Macromolecules* **2019**, *52*, 1985−1992.
(18) Qin, A.; Liu, Y.; Tang, B. Z. Regioselective Metal-Free Click Polymerization of Azides and Alkynes. *Macromol. Chem. Phys.* **2015**, *216*, 818−828.
(19) Li, B.; Huang, D.; Qin, A.; Tang, B. Z. Progress on Catalytic Systems Used in Click Polymerization. *Macromol. Rapid Commun.* **2018**, *39*, 1800098.
(20) Liu, Y.; Qin, A.; Tang, B. Z. Polymerizations Based on Triple-Bond Building Blocks. *Prog. Polym. Sci.* **2018**, *78*, 92−138.
(21) Han, T.; Deng, H.; Qiu, Z.; Zhao, Z.; Zhang, H.; Zou, H.; Leung, N. L. C.; Shan, G.; Elsegood, M. R. J.; Lam, J. W. Y.; Tang, B. Z. Facile Multicomponent Polymerizations toward Unconventional Luminescent Polymers with Readily Openable Small Heterocycles. *J. Am. Chem. Soc.* **2018**, *140*, 5588−5598.
(22) Tian, T.; Hu, R.; Tang, B. Z. Room Temperature One-Step Conversion from Elemental Sulfur to Functional Polythioureas through Catalyst-Free Multicomponent Polymerizations. *J. Am. Chem. Soc.* **2018**, *140*, 6156−6163.
(23) Xu, L.; Zhou, T.; Liao, M.; Hu, R.; Tang, B. Z. Multicomponent Polymerizations of Alkynes, Sulfonyl Azides, and 2-Hydroxybenzonitrile/2-Aminobenzonitrile toward Multifunctional Iminocoumarin/Quinoline-Containing Poly(N-sulfonylimine)s. *ACS Macro Lett.* **2019**, *8*, 101−106.
(24) Zhang, J.; Sun, J. Z.; Qin, A.; Tang, B. Z. Transition-Metal-Free Polymerization of Bromoalkynes and Phenols. *Macromolecules* **2019**, *52*, 2949−2955.
(25) Sun, X.-L.; Liu, D.-M.; Tian, D.; Zhang, X.-Y.; Wu, W.; Wan, W.-M. The Introduction of the Barbier Reaction into Polymer Chemistry. *Nat. Commun.* **2017**, *8*, 1210.
(26) Ji, Y.; Zhang, L.; Gu, X.; Zhang, W.; Zhou, N.; Zhang, Z.; Zhu, X. Sequence-Controlled Polymers with Furan-Protected Maleimide as a Latent Monomer. *Angew. Chem., Int. Ed.* **2017**, *56*, 2328−2333.
(27) Sun, Q.; Zhang, C.; Li, Z.; Kong, H.; Tan, Q.; Hu, A.; Xu, W. On-Surface Formation of One-Dimensional Polyphenylene through Bergman Cyclization. *J. Am. Chem. Soc.* **2013**, *135*, 8448−8451.
(28) Wang, Y.; Chen, S.; Hu, A. Chemical Synthesis of Carbon Nanomaterials Through Bergman Cyclization. In *From Polyphenylenes to Nanographenes and Graphene Nanoribbons*, Müllen, K., Feng, X., Eds.; Springer International Publishing: Cham, 2017.
(29) Sun, Z.; Huang, H.; Li, L.; Liu, L.; Chen, Y. Polythioamides of High Refractive Index by Direct Polymerization of Aliphatic Primary Diamines in the Presence of Elemental Sulfur. *Macromolecules* **2017**, *50*, 8505−8511.
(30) Zhao, B.; Gao, Z.; Zheng, Y.; Gao, C. Scalable Synthesis of Positively Charged Sequence-Defined Functional Polymers. *J. Am. Chem. Soc.* **2019**, *141*, 4541−4546.
(31) Chan, C. Y. K.; Tseng, N. W.; Lam, J. W. Y.; Liu, J.; Kwok, R. T. K.; Tang, B. Z. Construction of Functional Macromolecules with Well-Defined Structures by Indium-Catalyzed Three-Component Polycoupling of Alkynes, Aldehydes, and Amines. *Macromolecules* **2013**, *46*, 3246−3256.
(32) Liu, Y.; Gao, M.; Lam, J. W. Y.; Hu, R.; Tang, B. Z. Copper-Catalyzed Polycoupling of Diynes, Primary Amines, and Aldehydes: A New One-Pot Multicomponent Polymerization Tool to Functional Polymers. *Macromolecules* **2014**, *47*, 4908−4919.
(33) Zhang, Y.; Lam, J. W. Y.; Tang, B. Z. Palladium-Catalyzed Alkyne Polyannulation of Diphenols and Unactivated Internal Diynes: a New Synthetic Route to Functional Heterocyclic Polymers. *Polym. Chem.* **2016**, *7*, 330−338.
(34) Jayakannan, M.; Ramakrishnan, S. Recent Developments in Polyether Synthesis. *Macromol. Rapid Commun.* **2001**, *22*, 1463−1473.
(35) Wang, J.; Li, B.; Xin, D.; Hu, R.; Zhao, Z.; Qin, A.; Tang, B. Z. Superbase Catalyzed Regio-Selective Polyhydroalkoxylation of Alkynes: a Facile Route towards Functional Poly(vinyl ether)s. *Polym. Chem.* **2017**, *8*, 2713−2722.
(36) Mei, J.; Leung, N. L. C.; Kwok, R. T. K.; Lam, J. W. Y.; Tang, B. Z. Aggregation-Induced Emission: Together We Shine, United We Soar! *Chem. Rev.* **2015**, *115*, 11718−11940.
(37) Wu, Y.; Qin, A.; Tang, B. Z. AIE-active polymers for explosive detection. *Chin. J. Polym. Sci.* **2017**, *35*, 141−154.
(38) Qi, C.; Zheng, C.; Hu, R.; Tang, B. Z. Direct Construction of Acid-Responsive Poly(indolone)s through Multicomponent Tandem Polymerizations. *ACS Macro Lett.* **2019**, *8*, 569−575.
(39) Shi, H.; Kwok, R. T. K.; Liu, J.; Xing, B.; Tang, B. Z.; Liu, B. Real-Time Monitoring of Cell Apoptosis and Drug Screening Using Fluorescent Light-up Probe with Aggregation-Induced Emission Characteristics. *J. Am. Chem. Soc.* **2012**, *134*, 17972−17981.
(40) Hu, Y. B.; Lam, J. W. Y.; Tang, B. Z. Recent Progress in AIE-active Polymers. *Chin. J. Polym. Sci.* **2019**, *37*, 289−301.
(41) Yang, Z.; Chi, Z.; Mao, Z.; Zhang, Y.; Liu, S.; Zhao, J.; Aldred, M. P.; Chi, Z. Recent Advances in Mechano-Responsive Luminescence of Tetraphenylethylene Derivatives with Aggregation-Induced Emission Properties. *Mater. Chem. Front.* **2018**, *2*, 861−890.
(42) Liu, J.; Zhong, Y.; Lam, J. W. Y.; Lu, P.; Hong, Y.; Yu, Y.; Yue, Y.; Faisal, M.; Sung, H. H. Y.; Williams, I. D.; Wong, K. S.; Tang, B. Z. Hyperbranched Conjugated Polysiloles: Synthesis, Structure, Aggregation-Enhanced Emission, Multicolor Fluorescent Photopatterning, and Superamplified Detection of Explosives. *Macromolecules* **2010**, *43*, 4921−4936.
(43) Liu, J.; Lam, J. W. Y.; Jim, C. K. W.; Ng, J. C. Y.; Shi, J.; Su, H.; Yeung, K. F.; Hong, Y.; Faisal, M.; Yu, Y.; Wong, K. S.; Tang, B. Z. Thiol−Yne Click Polymerization: Regio- and Stereoselective Synthesis of Sulfur-Rich Acetylenic Polymers with Controllable Chain

DOI: 10.1021/acsmacrolett.9b00448
ACS Macro Lett. 2019, 8, 1068−1074

Conformations and Tunable Optical Properties. *Macromolecules* **2011**, *44*, 68−79.
(44) Gaudiana, R. A.; Minns, R. A. High Refractive Index Polymers. *J. Macromol. Sci., Chem.* **1991**, *28*, 831−842.
(45) Kasarova, S. N.; Sultanova, N. G.; Ivanov, C. D.; Nikolov, I. D. Analysis of the Dispersion of Optical Plastic Materials. *Opt. Mater.* **2007**, *29*, 1481−1490.

DOI: 10.1021/acsmacrolett.9b00448
ACS Macro Lett. 2019, 8, 1068−1074